

## Supporting information

### **A comparative study of two multi-resonance TADF analogous materials integrating chalcogen atoms of different periods**

Xin Xiong<sup>a</sup>, Ying-Chun Cheng<sup>a</sup>, Kai Wang<sup>ab\*</sup>, Jia Yu<sup>ac</sup> and Xiao-Hong Zhang<sup>ac\*</sup>

<sup>a</sup> *Institute of Functional Nano & Soft Materials (FUNSOM), Joint International Research Laboratory of Carbon-Based Functional Materials & Devices, Soochow University, Suzhou, Jiangsu 215123, P. R. China*

<sup>b</sup> *Jiangsu Key Laboratory for Carbon-Based Functional Materials & Devices, Soochow University, Suzhou, Jiangsu, 215123, PR China*

<sup>c</sup> *Jiangsu Key Laboratory of Advanced Negative Carbon Technologies, Soochow University, Suzhou, Jiangsu 215123, P. R. China*

E-mail: wkai@suda.edu.cn, xiaohong\_zhang@suda.edu.cn

## **General information**

$^1\text{H}$  NMR and  $^{13}\text{C}$  NMR spectra were recorded on a Bruker 600 spectrometer at room temperature. Mass spectra were recorded on a Thermo ISQ mass spectrometer using a direct exposure probe. UV-vis absorption spectra were recorded on a Hitachi U-3900 spectrophotometer. PL spectra and phosphorescent spectra were recorded on a Hitachi F-4600 fluorescence spectrophotometer. PL quantum efficiency was measured by an absolute PL quantum yield measurement system (C11347-01, Hamamatsu Photonics) under the flow of nitrogen gas with an excitation wavelength of 300 nm. Transient PL decay was measured using a Quantaaurus-Tau spectrometer (C16361-01, Hamamatsu Photonics) under vacuum condition.

Cyclic voltammetry (CV) was carried out on a CHI660E electrochemical analyzer at room temperature. Dry DCM was used as solvent with tetrabutylammonium hexafluorophosphate ( $\text{TBAPF}_6$ ) (0.1 M) as the supporting electrolyte. The cyclic voltammograms (CV) were obtained at scan rate of  $0.05 \text{ V}\cdot\text{S}^{-1}$  with platinum electrode as the working/counter electrode and an  $\text{Ag}/\text{AgNO}_3$  electrode as the reference electrode with standardized against ferrocene/ferrocenium.

## **Theoretical calculations**

All the calculations are performed using Gaussian 09 program package. Theoretical calculations of the ground state are performed by using density functional theory (DFT) at the level of PBE1PBE/6-31g (d, p) set.

## **Device fabrication and measurement**

The OLEDs were fabricated on the indium-tin oxide (ITO) coated transparent glass

substrates, the ITO conductive layer has a thickness of ca. 100 nm and a sheet resistance of ca. 30  $\Omega$  per square. The substrates were cleaned with ethanol, acetone and deionized water, and then dried in an oven, finally exposed to UV ozone for 15 min. All of the organic materials and metal layers were thermal evaporated under a vacuum of ca.  $10^{-5}$  Torr. Four identical OLED devices were formed on each of the substrates and the emission area of 0.09 cm<sup>2</sup> for each device. The EL performances of the devices were measured with a PHOTO RESEARCH Spectra Scan PR 655 PHOTOMETER and a KEITHLEY 2400 Source Meter constant current source at room temperature.

## **Experimental**

### **Synthesis**

All the chemicals and reagents used in this work were purchased from commercially without further purification.

#### **Synthesis of 9-(3-bromo-2-chlorophenyl)-3,6-di-tert-butyl-9H-carbazole (Cz-Cl-Br).**

Under nitrogen atmosphere, to a 500 mL round-bottom flask equipped with magnetic stirring bar and reflux condenser, 1-Bromo-2chloro-3-fluorobenzene (8.38 g, 40 mmol), 3,6-Di-tert-butylcarbazole (13.42 g, 48 mmol), Cs<sub>2</sub>CO<sub>3</sub> (26.1 g, 80 mmol) and anhydrous DMF (300 mL) were added. The mixture was stirred at 160°C for 24h, then cooled down to room temperature. The reaction mixture was poured into ice water (2 L), and the white solid was collected by filtration. The crude product was purified via column chromatography eluting with petroleum ether-dichloromethane (10:1, v/v)

mixtures to afford white solid. (15.89 g, yield: 84.7%). <sup>1</sup>H NMR (400 MHz, CD<sub>2</sub>Cl<sub>2</sub>): δ 8.21 (d, J = 1.9 Hz, 2H), 7.72 (dd, J = 8.1, 1.6 Hz, 1H), 7.51 (dd, J = 8.6, 1.9 Hz, 3H), 7.43 (dd, J = 7.8, 1.6 Hz, 1H), 7.01 (d, J = 8.6 Hz, 2H), 1.50 (s, 18H). <sup>13</sup>C NMR (101 MHz, CDCl<sub>3</sub>): δ 143.16, 139.14, 137.31, 134.56, 133.61, 129.72, 128.34, 124.56, 123.74, 123.41, 116.40, 109.42, 34.80, 32.07. MALDI-TOF: Calculated: 468.86, Found: 468.34. Anal. Calcd (%) for C<sub>26</sub>H<sub>27</sub>BrClN: C, 66.60; H, 5.80; Br, 17.04; Cl, 7.56; N, 2.99; Found: C, 66.52; H, 5.62; N, 2.91.

**Synthesis of 10-(2-chloro-3-(3,6-di-tert-butyl-9H-carbazol-9-yl)phenyl)-10H-phenoxazine (Cz-Cl-PXZ).**

In a 250 mL round flask, a mixture of Phenoxazine (3.3 g, 18.0 mmol), Cz-Cl-Br (7 g, 15.0 mmol), Pd(OAc)<sub>2</sub> (125 mg, 0.75 mmol), (*t*-Bu)<sub>3</sub>PHBF<sub>4</sub> (435 mg, 1.50 mmol), *t*-BuONa (5.77 g, 60 mmol) and 125 mL toluene was stirred and refluxed at 110 °C under N<sub>2</sub> atmosphere for 24 hours. The reaction was then quenched by water and extracted with dichloromethane. After evaporation of the solvent, the residue was purified via column chromatography by using petroleum ether/dichloromethane (10:1, v/v) as eluent to afford white solid (6.43 g, yield: 75%). <sup>1</sup>H NMR (400 MHz, CDCl<sub>3</sub>) δ 8.17 (dd, J = 1.9, 0.7 Hz, 2H), 7.66 (s, 3H), 7.49 (dd, J = 8.6, 1.9 Hz, 2H), 7.06 (dd, J = 8.6, 0.6 Hz, 2H), 6.77 – 6.69 (m, 6H), 6.01 – 5.94 (m, 2H), 1.48 (s, 18H). <sup>13</sup>C NMR (101 MHz, CDCl<sub>3</sub>) δ 143.91, 143.28, 139.10, 138.66, 137.88, 135.82, 132.90, 132.70, 131.18, 129.60, 123.85, 123.59, 123.57, 121.99, 116.53, 115.88, 112.66, 109.40, 34.85,

32.11. MALDI-TOF: Calculated: 571.16, Found: 571.42. Anal. Calcd (%) for  $C_{38}H_{35}ClN_2O$ : C, 79.91; H, 6.18; Cl, 6.21; N, 4.90; Found: C, 79.81; H, 6.12; N, 3.92.

### Synthesis of BNCzPXZ.

A solution of tert-butyllithium in pentane (15.3 mL, 1.30 M, 20.0 mmol) was added slowly to a solution of Cz-Cl-PXZ (5.71 g, 10.0 mmol) in tert-butylbenzene (100 mL) at 0 °C under a nitrogen atmosphere. After stirring at 60 °C for 2 h, pentane was removed in vacuo. After addition of boron tribromide (1.9 mL, 20.0 mmol) at -40 °C, the reaction mixture was stirred at room temperature for 1 h. N,N-Diisopropylethylamine (3.4 mL, 20.0 mmol) was added at 0 °C and then the reaction mixture was allowed to warm to room temperature. After stirring at 150 °C for 8 h, the reaction mixture was cooled to room temperature. 10 mL methanol was added to the reaction mixture to quench residual  $BBr_3$ . The aqueous layer was separated and extracted with dichloromethane (50 mL $\times$ 3). The organic phase was collected and dried by anhydrous  $Na_2SO_4$ , and then the solvent was evaporated. The residue was purified via column chromatography eluting with petroleum ether-dichloromethane (30:1, v/v) mixtures to afford yellow solid. (0.98 g, yield 18%).  $^1H$  NMR (400 MHz,  $CD_2Cl_2$ )  $\delta$  8.84, 8.54, 8.54, 8.40, 8.40, 8.38, 8.37, 8.35, 8.34, 8.34, 8.33, 8.23, 8.22, 8.21, 8.20, 7.86, 7.85, 7.84, 7.73, 7.73, 7.72, 7.71, 7.70, 7.69, 7.35, 7.33, 7.32, 7.26, 7.24, 7.20, 7.18, 7.17, 7.15, 7.13, 7.08, 7.08, 7.06, 7.04, 1.66, 1.57.  $^{13}C$  NMR (101 MHz,  $CD_2Cl_2$ )  $\delta$  149.41, 147.20, 145.38, 144.87, 143.08, 142.79, 138.15, 136.96, 132.06, 131.39, 129.42, 129.34, 126.86, 125.36, 124.46, 123.52, 123.30, 123.19, 120.78, 118.75, 117.54, 117.29, 116.96,

113.97, 109.73, 106.91, 35.07, 34.68, 31.93, 31.61, 31.55. MALDI-TOF: Calculated: 544.51, Found: 544.12. Anal. Calcd (%) for C<sub>38</sub>H<sub>33</sub>BN<sub>2</sub>O: C, 83.82; H, 6.11; B, 1.99; N, 5.14; O, 2.94; Found: C, 83.72; H, 6.02; N, 5.08.

**Synthesis of 10-(2-chloro-3-(3,6-di-tert-butyl-9H-carbazol-9-yl)phenyl)-10H-phenothiazine (Cz-Cl-PTZ).**

The synthetic process was in the same way as 10-(2-chloro-3-(3,6-di-tert-butyl-9H-carbazol-9-yl)phenyl)-10H-phenoxazine (Cz-Cl-PXZ), but phenoxazine was replaced with equivalent stoichiometric amounts of phenothiazine. Yellow solid (6.87 g, yield: 78%). <sup>1</sup>H NMR (400 MHz, CD<sub>2</sub>Cl<sub>2</sub>) δ 8.47 (d, J = 2.1 Hz, 2H), 7.89 – 7.79 (m, 3H), 7.74 (dd, J = 8.6, 1.9 Hz, 2H), 7.32 (d, J = 8.7 Hz, 2H), 7.20 – 7.10 (m, 4H), 7.01 (td, J = 7.5, 1.2 Hz, 2H), 6.44 (dd, J = 8.2, 1.3 Hz, 2H), 1.70 (d, J = 2.3 Hz, 18H). Anal. Calcd (%) for C<sub>38</sub>H<sub>35</sub>ClN<sub>2</sub>S: C, 77.72; H, 6.01; Cl, 6.04; N, 4.77; S, 5.46; Found: C, 77.62; H, 5.92; N, 4.58; S, 5.28.

**Synthesis of BNCzPTZ.**

The same way as BNCzPXZ, but Cz-Cl-PXZ was replaced with equivalent stoichiometric amounts of Cz-Cl-PTZ. Yellow solid (1.12g yield: 20%). <sup>1</sup>H NMR (400 MHz, CD<sub>2</sub>Cl<sub>2</sub>) δ 8.71 (d, J = 1.9 Hz, 1H), 8.45 – 8.38 (m, 2H), 8.27 – 8.20 (m, 2H), 8.11 (d, J = 8.2 Hz, 1H), 7.67 (t, J = 8.3 Hz, 1H), 7.58 (dd, J = 8.8, 2.1 Hz, 1H), 7.44 (dd, J = 7.6, 1.3 Hz, 2H), 7.36 – 7.31 (m, 1H), 7.27 (t, J = 7.5 Hz, 1H), 7.19 (dd, J = 7.5, 1.9 Hz, 1H), 7.07 – 6.98 (m, 2H), 1.53 (s, 9H), 1.43 (s, 9H). <sup>13</sup>C NMR (101 MHz, CDCl<sub>3</sub>) δ 147.16, 146.41, 145.28, 144.88, 143.11, 142.28, 141.81, 138.22, 133.83,

132.13, 129.44, 129.37, 128.68, 128.64, 127.19, 126.98, 125.42, 124.67, 124.46, 123.75, 123.69, 122.48, 120.82, 117.24, 114.04, 112.73, 107.34, 35.21, 34.83, 32.27, 31.88. MALDI-TOF: Calculated: 560.57, Found: 560.17. Anal. Calcd (%) for  $C_{38}H_{33}BN_2S$ : C, 81.42; H, 5.93; B, 1.93; N, 5.00; S, 5.72; Found: C, 82.33; H, 5.79; N, 4.87; S, 5.66.

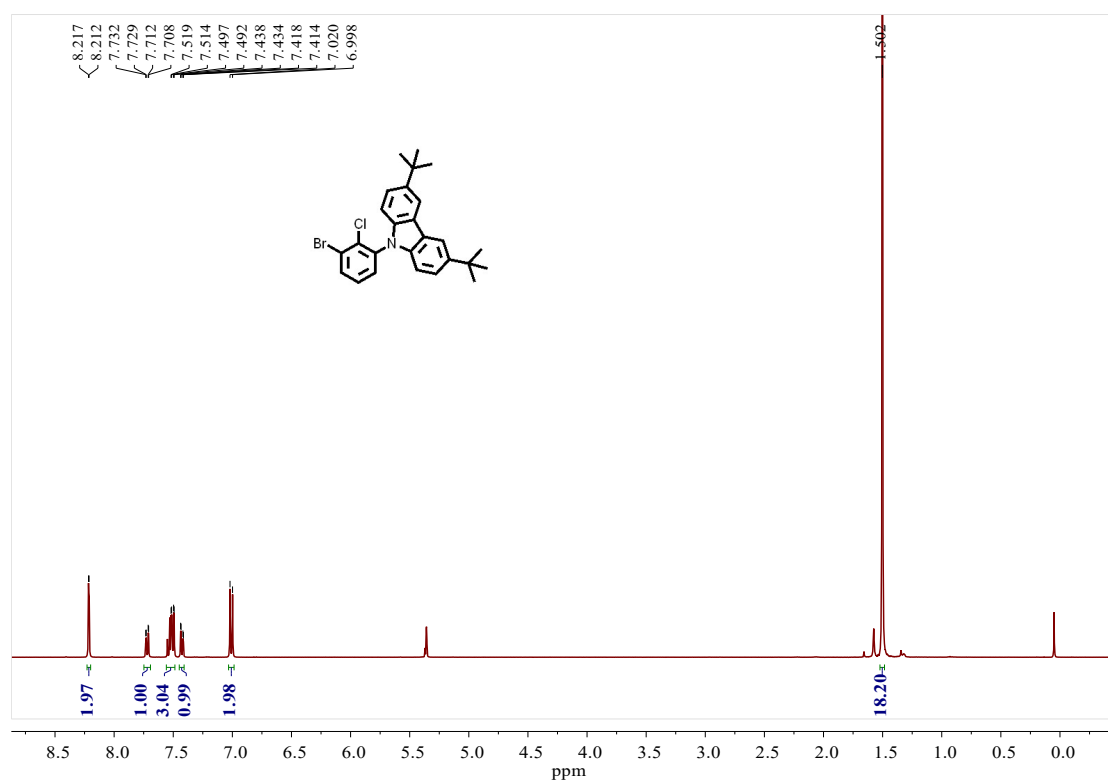


**Figure S1.**  $^1H$  NMR spectrum ( $CD_2Cl_2$ , 400 MHz) of Cz-Cl-Br.

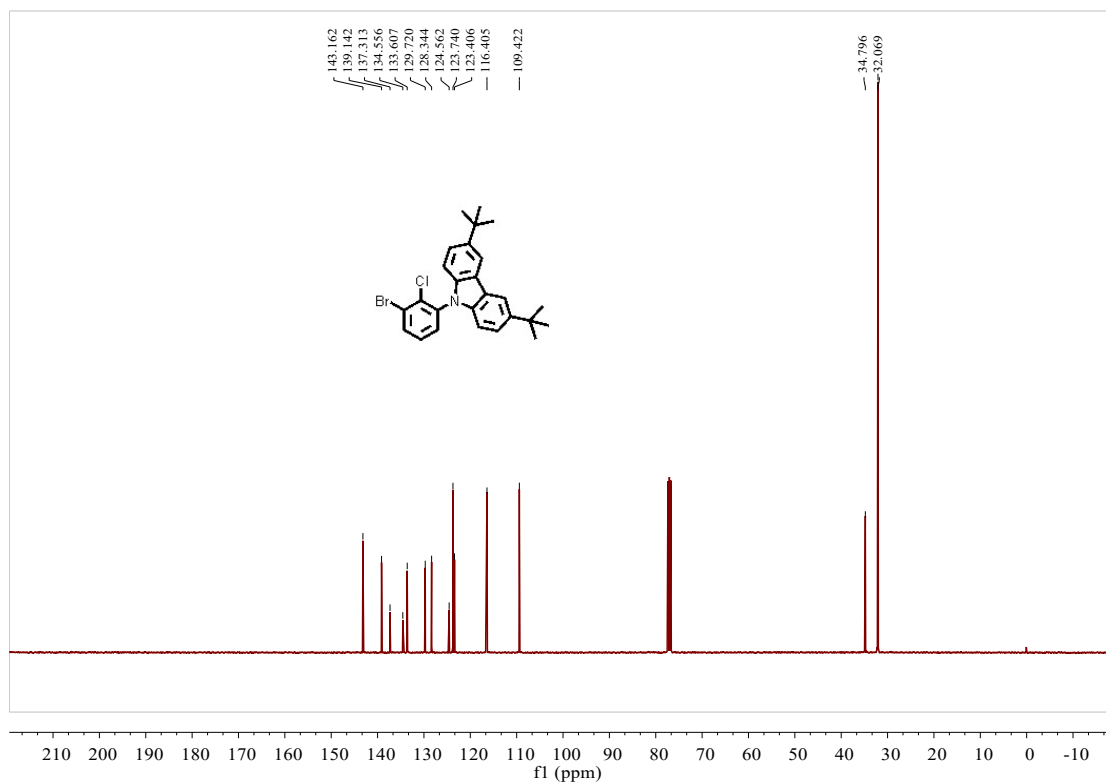


**Figure S2.** <sup>13</sup>C NMR spectrum (CDCl<sub>3</sub>, 101 MHz) of Cz-Cl-Br.

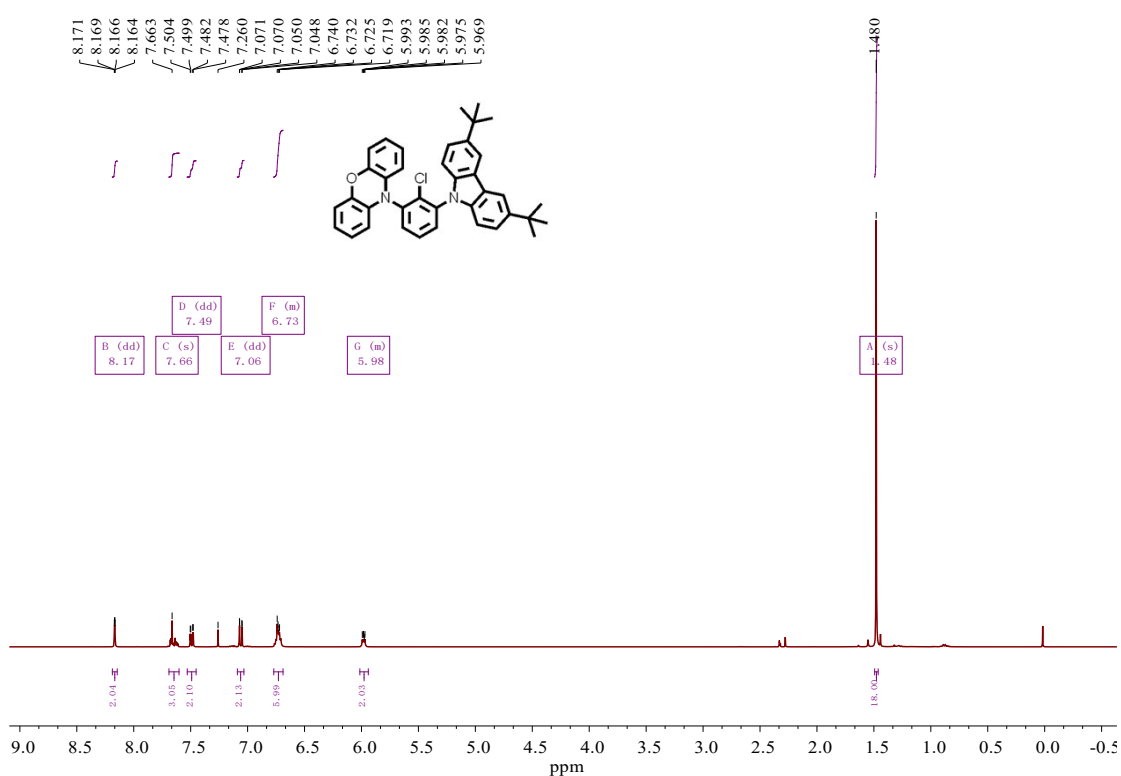


**Figure S3.** <sup>1</sup>H NMR spectrum (CDCl<sub>3</sub>, 400 MHz) of Cz-Cl-PXZ.



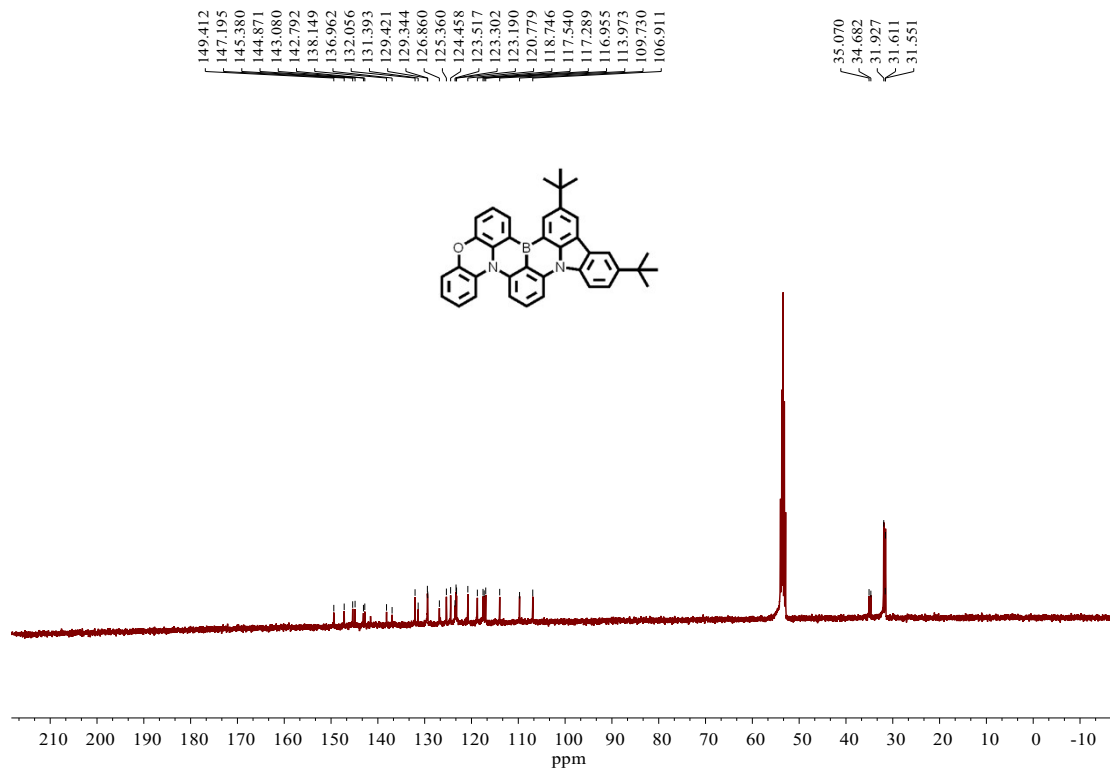


**Figure S6.** <sup>13</sup>C NMR spectrum (101 MHz, CD<sub>2</sub>Cl<sub>2</sub>) of BNCzPXZ.

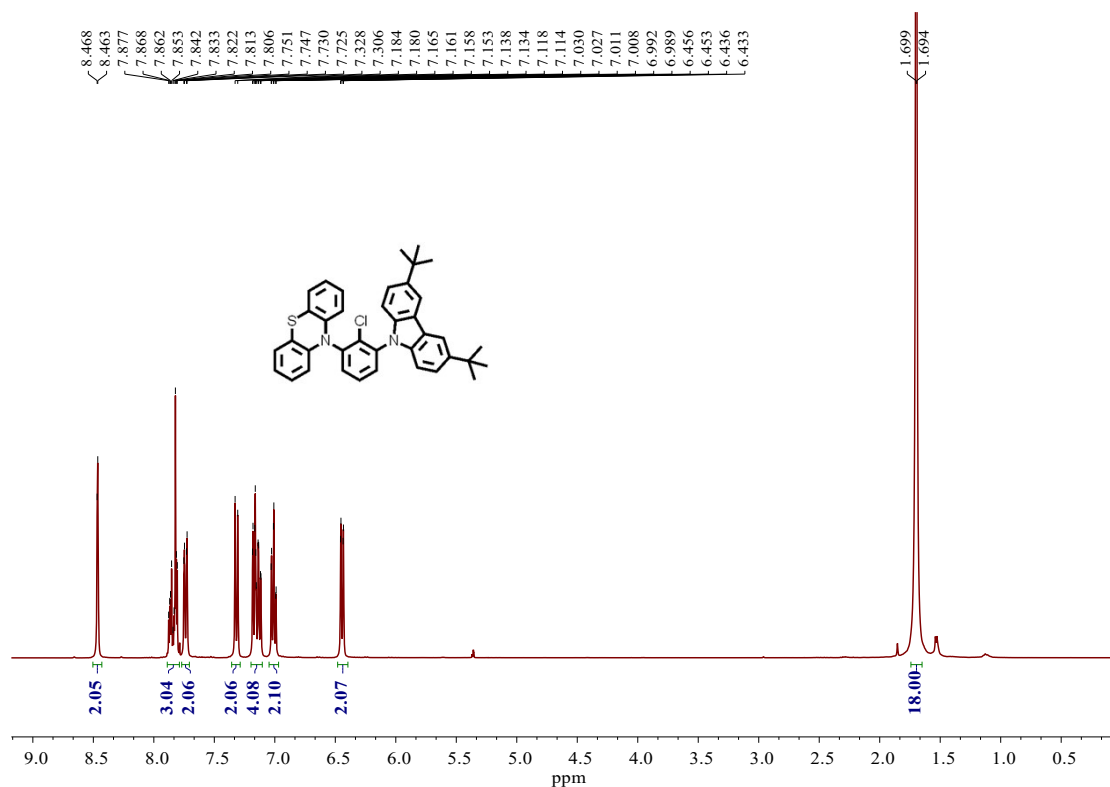


**Figure S7.** <sup>1</sup>H NMR spectrum (CD<sub>2</sub>Cl<sub>2</sub>, 400 MHz) of Cz-Cl-PTZ.

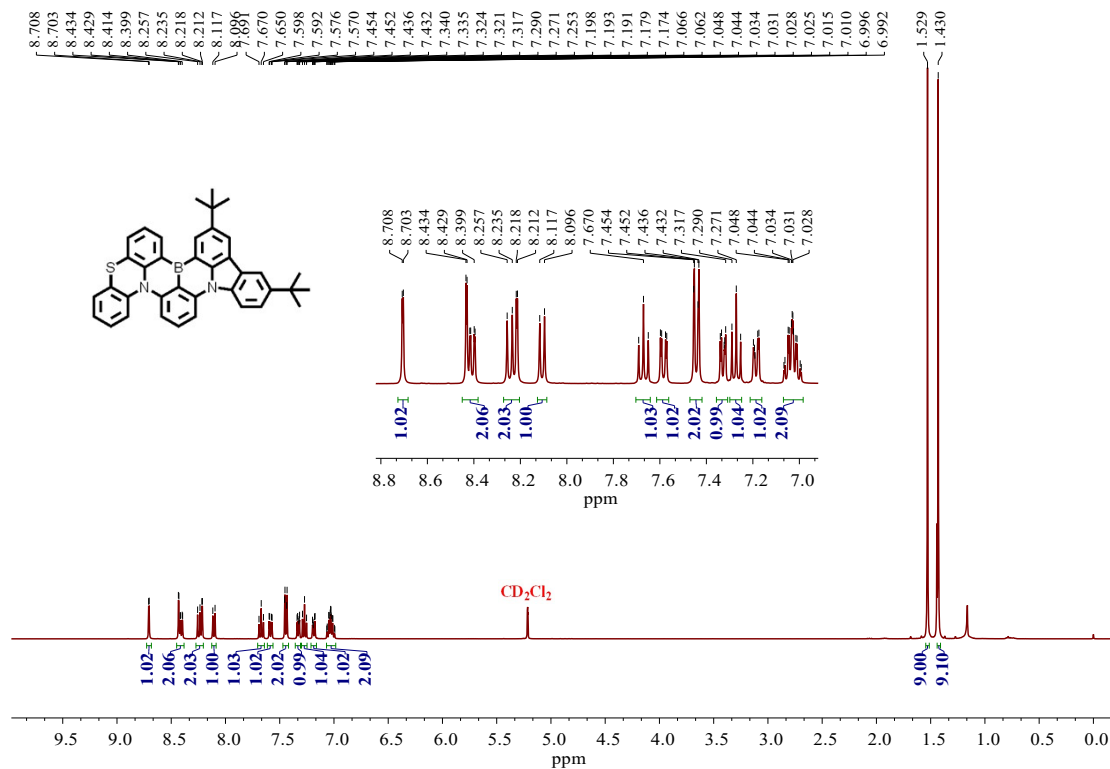


**Figure S8.**  $^1\text{H}$  NMR spectrum ( $\text{CD}_2\text{Cl}_2$ , 400 MHz) of BNCzPTZ.

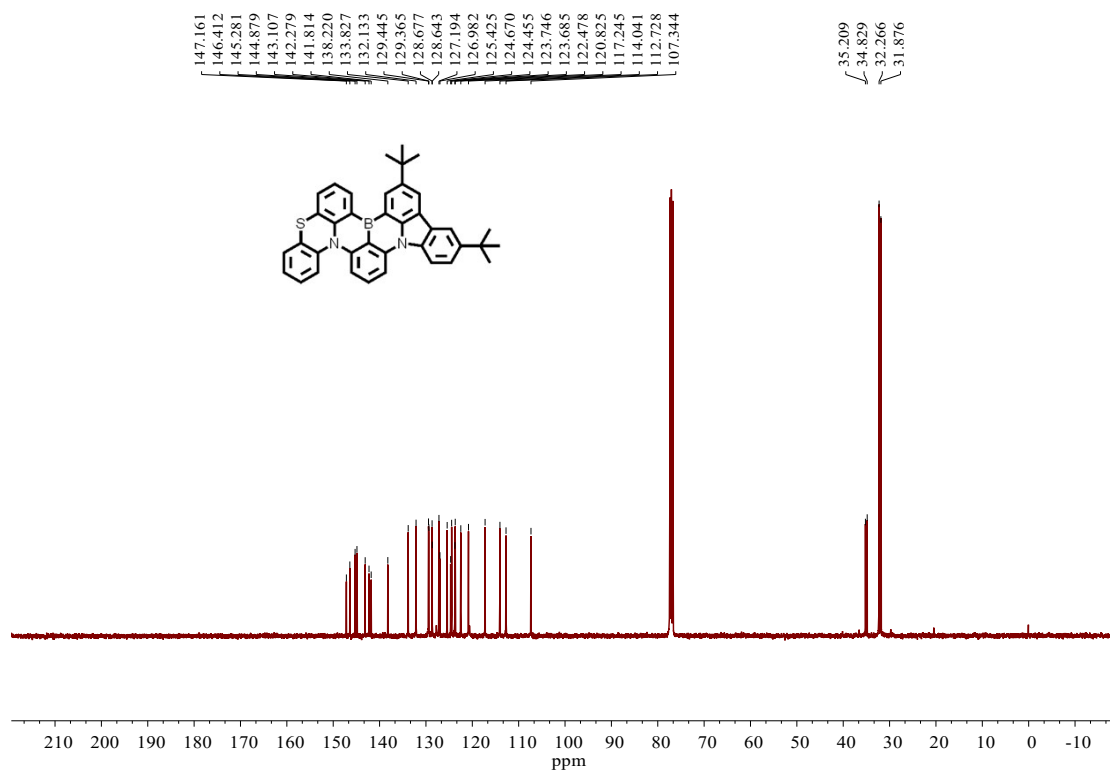


**Figure S9.**  $^{13}\text{C}$  NMR spectrum (101 MHz,  $\text{CDCl}_3$ ) of BNCzPTZ.

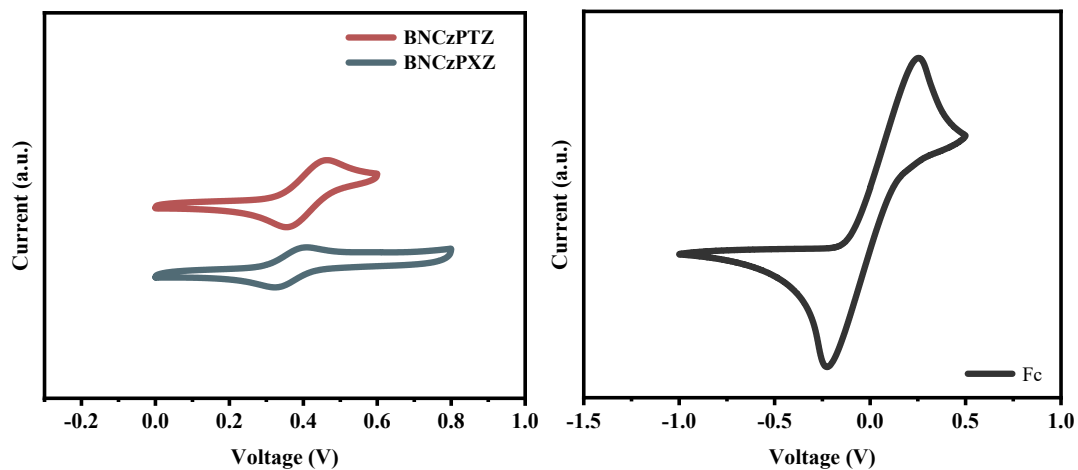


**Figure S10.** Cyclic voltammogram curves of BNCzPXZ and BNCzPTZ.

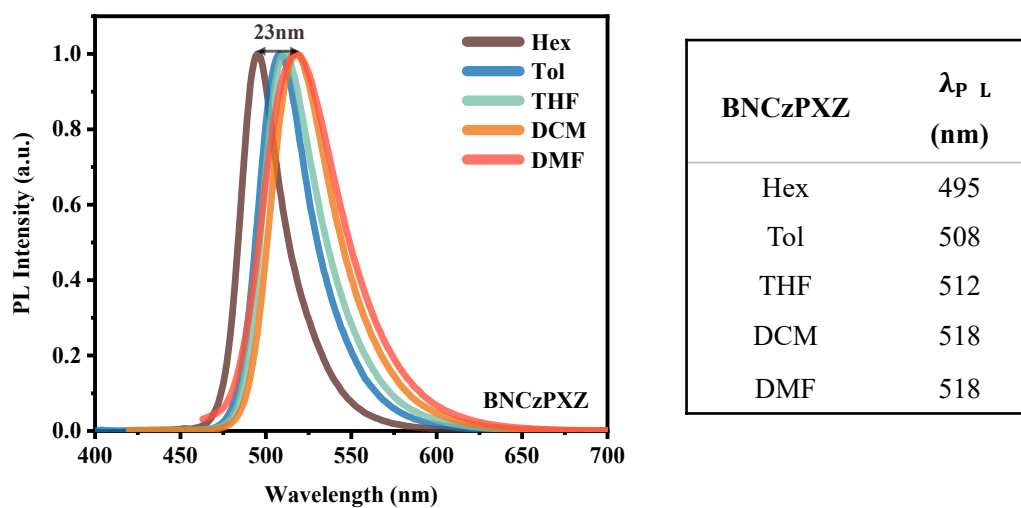
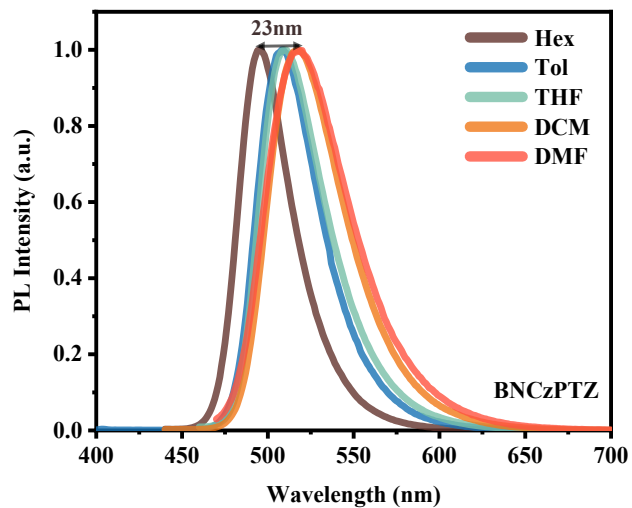


**Figure S11.** Photophysical properties of BNCzPXZ in various solutions with different polarities.



<b>BNCzPTZ</b>	$\lambda_{pL}$ <b>(nm)</b>
Hex	495
Tol	509
THF	510
DCM	517
DMF	518

**Figure S12.** Photophysical properties of BNCzPTZ in various solutions with different polarities.

**Table S1.** Kinetic parameters of BNCzPXZ, and BNCzPTZ doped in 7wt% and 15wt% PhCzBCz films, respectively.

Compound	$\Phi_{PL}$ [%]	$\tau_{PF}/\tau_{DF}$ [ns/ $\mu$ s]	$\Phi_P/\Phi_D$	$k_{ISC}$ [ $10^7 \text{ s}^{-1}$ ]	$k_{RISC}$ [ $10^4 \text{ s}^{-1}$ ]	$k_r$ [ $10^7 \text{ s}^{-1}$ ]
BNCzPXZ	94	10.76/102.41	0.382/0.558	5.74	2.31	3.55
BNCzPTZ	91	39.43/33.35	0.172/0.738	2.11	15.4	0.439

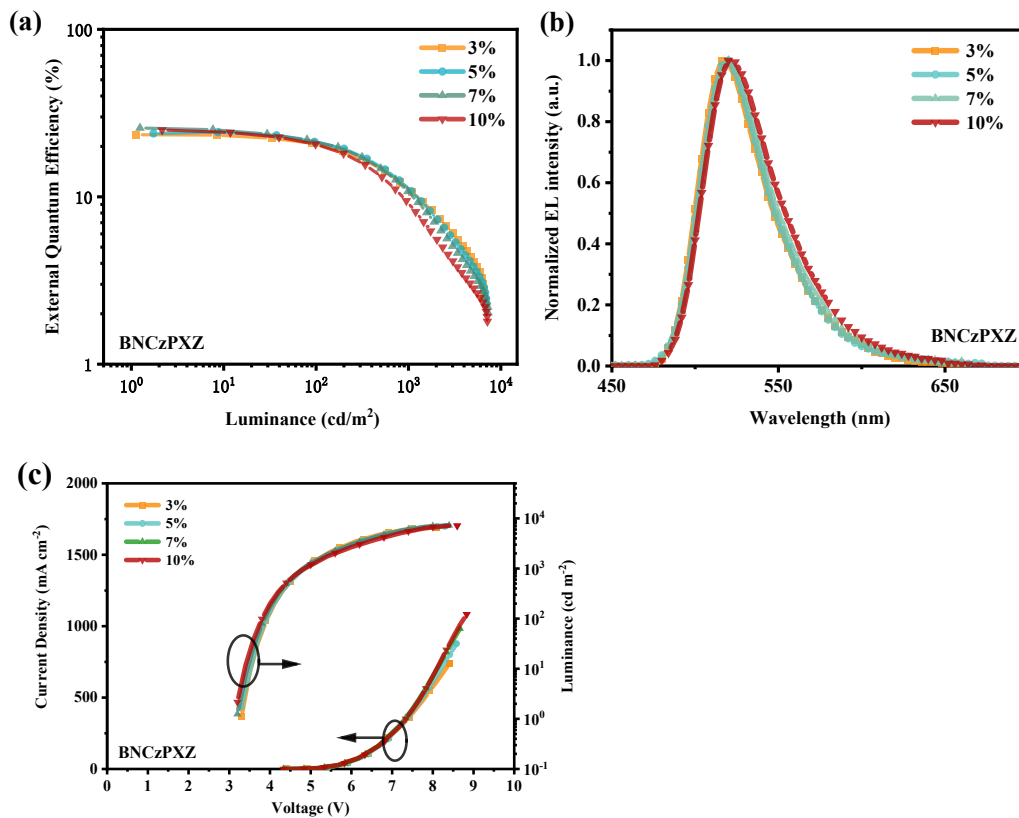
## Electroluminescence properties

**Table S2.** EL performances of the devices based on BNCzPXZ.

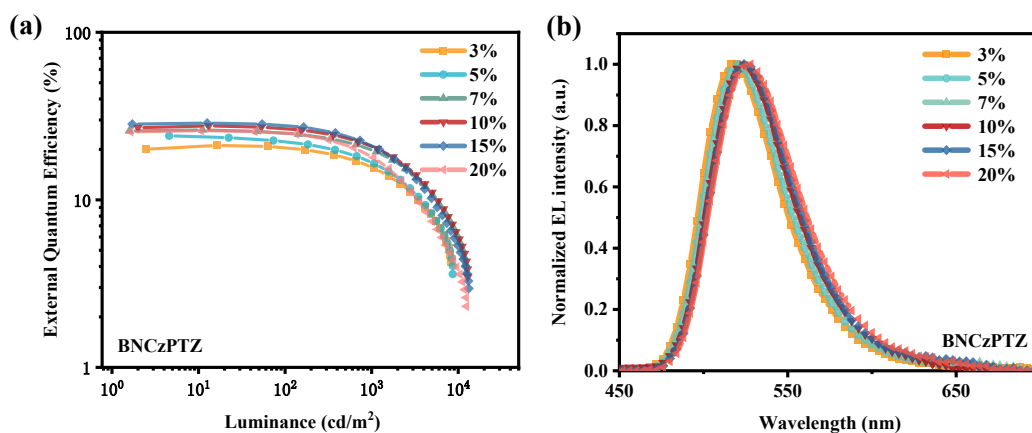
TAPC(30)/TCTA(10)/mCP(10)/PhCzBCz:BNCzPXZ(20)/TmPyPb(40)/LiF(1)/Al							
Concentration	$\lambda_{max}$ (nm)	FWHM (nm)	$L_{max}$ ( $\text{cd m}^{-2}$ )	$CE_{max}$ ( $\text{cd A}^{-1}$ )	$PE_{max}$ ( $\text{lm W}^{-1}$ )	$EQE_{max 100 1000}$ (%)	CIE
3%	516	48	6515	81.9	77.9	23.5/20.8/10.6	(0.24, 0.68)
5%	520	48	6949	84.9	76.2	24.3/21.3/10.8	(0.24, 0.67)
7%	<b>520</b>	<b>49</b>	<b>7262</b>	<b>93.7</b>	<b>91.9</b>	<b>25.7/21.1/10.4</b>	<b>(0.25, 0.67)</b>
10%	520	52	7150	91.9	90.2	25.0/20.6/8.1	(0.26, 0.67)

**Table S3.** EL performances of the devices based on BNCzPTZ.

TAPC(30)/TCTA(10)/mCP(10)/PhCzBCz:BNCzPTZ(20)/TmPyPb(40)/LiF(1)/Al							
Concentration	$\lambda_{max}$ (nm)	FWHM (nm)	$L_{max}$ ( $\text{cd m}^{-2}$ )	$CE_{max}$ ( $\text{cd A}^{-1}$ )	$PE_{max}$ ( $\text{lm W}^{-1}$ )	$EQE_{max 100 1000}$ (%)	CIE
3%	520	54	8227	72.8	65.3	21.1/20.4/15.5	(0.23, 0.66)
5%	520	55	8656	85.5	81.4	24.1/22.2/16.5	(0.25, 0.66)
7%	524	56	12370	93.7	89.2	26.1/25.3/19.5	(0.26, 0.66)
10%	524	56	12920	97.5	92.8	27.6/26.8/20.4	(0.26, 0.65)
<b>15%</b>	<b>524</b>	<b>57</b>	<b>13240</b>	<b>105.0</b>	<b>103.0</b>	<b>28.7/27.9/20.7</b>	<b>(0.27, 0.65)</b>
20%	528	59	12450	95.8	97	25.8/25.2/17.8	(0.28, 0.66)



**Figure S13.** EL characteristics of the OLEDs with the configuration of [ITO/TAPC (30 nm)/TCTA (10 nm)/mCP (10 nm)/PhCzBCz: BNCzPXZ (20 nm)/TmTyPB (40 nm)/LiF (1 nm)/Al (120 nm)]. (a) EQE-*L* curves. (b) EL spectra. (c) *J-V-L* curves.



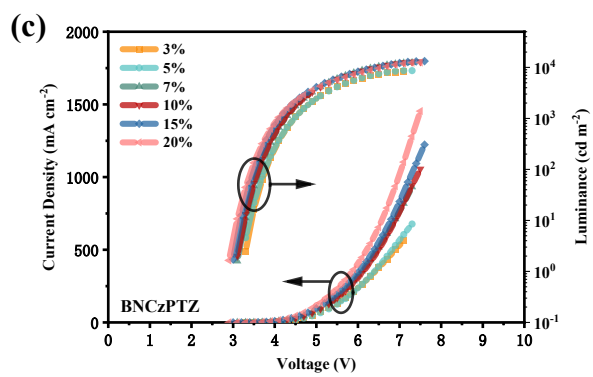


**Figure S14.** EL characteristics of the OLEDs with the configuration of [ITO/TAPC (30 nm)/TCTA (10 nm)/mCP (10 nm)/PhCzBCz: BNCzPTZ (20 nm)/TmTyPB (40 nm)/LiF (1 nm)/Al (120 nm)]. (a) EQE-*L* curves. (b) EL spectra. (c) *J-V-L* curves.